



Pergamon

Progress in Oceanography 53 (2002) 115–139

**Progress in  
Oceanography**

[www.elsevier.com/locate/pocean](http://www.elsevier.com/locate/pocean)

## The Northern Oscillation Index (NOI): a new climate index for the northeast Pacific

F.B. Schwing<sup>a,\*</sup>, T. Murphree<sup>b</sup>, P.M. Green<sup>c</sup>

<sup>a</sup> Southwest Fisheries Science Center NOAA NMFS, Pacific Fisheries Environmental Laboratory, 1352 Lighthouse Avenue, Pacific Grove, CA 93950-2097, USA

<sup>b</sup> Department of Meteorology, Naval Postgraduate School, Monterey, CA 93943-5114, USA

<sup>c</sup> Joint Institute of Marine and Atmospheric Research, University of Hawaii, 1000 Pope Road, MSB 312, Honolulu, HI 96822, USA

---

### Abstract

We introduce the Northern Oscillation Index (NOI), a new index of climate variability based on the difference in sea level pressure (SLP) anomalies at the North Pacific High (NPH) in the northeast Pacific (NEP) and near Darwin, Australia, in a climatologically low SLP region. These two locations are centers of action for the north Pacific Hadley–Walker atmospheric circulation. SLPs at these sites have a strong negative correlation that reflects their roles in this circulation. Global atmospheric circulation anomaly patterns indicate that the NEP is linked to the western tropical Pacific and southeast Asia via atmospheric wave trains associated with fluctuations in this circulation. Thus the NOI represents a wide range of tropical and extratropical climate events impacting the north Pacific on intraseasonal, interannual, and decadal scales. The NOI is roughly the north Pacific equivalent of the Southern Oscillation Index (SOI), but extends between the tropics and extratropics. Because the NOI is partially based in the NEP, it provides a more direct indication of the mechanisms by which global-scale climate events affect the north Pacific and North America.

The NOI is dominated by interannual variations associated with El Niño and La Niña (EN/LN) events. Large positive (negative) index values are usually associated with LN (EN) and negative (positive) upper ocean temperature anomalies in the NEP, particularly along the North American west coast. The NOI and SOI are highly correlated, but are clearly different in several respects. EN/LN variations tend to be represented by larger swings in the NOI. Forty percent of the interannual moderate and strong interannual NOI events are seen by the SOI as events that are either weak or opposite in sign. The NOI appears to be a better index of environmental variability in the NEP than the SOI, and NPH SLP alone, suggesting the NOI is more effective at incorporating the influences of regional and remotely teleconnected climate processes.

The NOI contains alternating decadal-scale periods dominated by positive and negative values, suggesting substantial climate shifts on a roughly 14-year ‘cycle’. The NOI was predominantly positive prior to 1965, during 1970–1976 and 1984–1991, and since 1998. Negative values predominated in 1965–1970, 1977–1983, and 1991–1998. In the NEP, interannual and decadal-scale negative NOI periods (e.g. EN events) are generally associated with weaker trade winds, weaker coastal upwelling-favorable winds, warmer upper ocean temperatures, lower Pacific Northwest salmon catch, higher Alaska salmon catch, and generally decreased macrozooplankton biomass off southern California. The opposite physical and biological patterns generally occur when the index is positive. Simultaneous correlations of the NOI with

---

\* Corresponding author. Tel.: +1-831-648-9034; fax: 831-648-8440.

E-mail address: [fschwing@pfeg.noaa.gov](mailto:fschwing@pfeg.noaa.gov) (F.B. Schwing).

north Pacific upper ocean temperature anomalies are greatest during the boreal winter and spring. Lagged correlations of the winter and spring NOI with subsequent upper ocean temperatures are high for several seasons. The relationships between the NOI and atmospheric and physical and biological oceanic anomalies in the NEP indicate this index is a useful diagnostic of climate change in the NEP, and suggest mechanisms linking variations in the physical environment to marine resources on interannual to decadal climate scales. The NOI time series is available online at: <http://www.pfeg.noaa.gov>. © 2002 Elsevier Science Ltd. All rights reserved.

## Contents

1. Introduction . . . . .	116
1.1. Why a new index? . . . . .	119
1.2. The 1997–1998 El Niño event . . . . .	120
2. Data and methods . . . . .	121
3. Results . . . . .	122
3.1. Comparison of index time series . . . . .	122
3.2. Global correlation maps . . . . .	125
3.3. Pacific basin anomaly fields . . . . .	128
3.4. Correlation with northeast Pacific Ocean time series . . . . .	132
4. Discussion . . . . .	134
4.1. El Niño, La Niña and teleconnections . . . . .	135
4.2. The NOI as an index of physical and biological variability . . . . .	135
5. Conclusions . . . . .	136

## 1. Introduction

Climate change processes act on many time scales, from El Niño/La Niña (EN/LN) cycles to decadal and longer. They also act on a range of spatial scales, from global down to local ecosystems. Climate change in the northeast Pacific (NEP) is linked to major ecological fluctuations, including changes in salmon populations (Beamish, 1993; Finney, Gregory-Eaves, Sweetman, Douglas, & Smol, 2000; Francis & Hare, 1994; Mantua, Hare, Zhang, Wallace, & Francis, 1997; Pulwarty & Redmond, 1997) and other marine organisms (Brodeur & Ware, 1992; McFarlane, King, & Beamish, 2000; Polovina et al., 1994; Roemmich & McGowan, 1995; Schwing, Moore, Ralston, & Sakuma, 2000).

Many climate variations occur via atmospheric and oceanic teleconnections (Horel & Wallace, 1981; Nitta, 1987; Schwing, Murphree, deWitt & Green, 2002). The cause and effect relationships between teleconnections in the atmosphere and ocean are not well understood (Mantua et al., 1997; Pulwarty & Redmond, 1997). However, the anomaly patterns for many intraseasonal to decadal events are consistent with anomalous atmospheric forcing of the ocean (Miller, Cayan, Barnett, Graham, & Oberhuber, 1994; Parrish, Schwing, & Mendelssohn, 2000; Simpson, 1992). Atmospheric teleconnections extend from the troposphere to the surface and include distinct fluctuations in sea level pressure (SLP) (Schwing et al., 2002). SLP changes are closely linked to changes in surface winds, and thereby to changes in sea surface temperature (SST), upper ocean temperature and heat content, mixed layer depth, and thermocline depth (Cayan, 1992; Gill, 1982; Miller et al., 1994; Schwing et al., 2002). Through these links, SLP plays an

important role in influencing and defining ocean climate change. It is also relatively well observed and analyzed. Thus SLP can be used to construct useful indices for assessing climate changes in the atmosphere and ocean.

To track EN, LN, and other climate events, a number of SLP-based indices have been created; for example, the Southern Oscillation Index (SOI) (Trenberth & Shea, 1987), the North Atlantic Oscillation (NAO) Index (Barnston & Livezey, 1987; Hurrell, 1995), and the North Pacific (NP) Index (Trenberth & Hurrell, 1994). The best known of these is the SOI, which is based on the SLP anomaly (SLPA) difference between a site in the tropical or subtropical southeast Pacific, usually Tahiti, and one in the western tropical Pacific, usually Darwin, Australia (Chelliah, 1990; Chen, 1982). These locations are used because the oscillation described by them represents, or is correlated with, a number of climate variations occurring in and well beyond the tropical Pacific (Horel & Wallace, 1981; Trenberth & Shea, 1987; Walker, 1924). Tahiti and Darwin are commonly used in part because they have fairly reliable SLP data that extend back for several decades, a rarity in this region.

The sites used in computing the SOI are near the tropical and subtropical centers of action for the south Pacific Hadley–Walker (H–W) circulation (Bjerknes, 1966, 1969), a major atmospheric pathway for the transport of mass, momentum, and energy between the tropics and extratropics (Peixoto & Oort, 1992). The H–W circulation, which extends throughout the troposphere, has a meridional component (the Hadley circulation, after Hadley, 1735) and a zonal component (the Walker circulation, after Walker, 1924). Fig. 1 shows schematically the Pacific portion of the mean H–W circulation. The major features are a large region of low SLP in the western tropical Pacific-southeast Asian region coupled by lower and upper tropospheric winds to two areas of high SLP in the extratropics; the North Pacific High (NPH) in the NEP and the South Pacific High (SPH) in the southeast Pacific. Through this circulation, the NPH and SPH participate in climate variations of southeast Asia and the tropical Indo-Pacific region. On intraseasonal to interannual scales, SLP variations at the NPH and SPH tend to be out-of-phase with the western tropical Pacific-southeast Asia (Fig. 2a).

Variations in SLP at these locations, and in the winds that link these regions, reflect a variety of climate processes (cf. Schwing et al., 2002). Through these processes, the NEP is strongly linked to atmospheric and oceanic changes occurring outside the north Pacific region; for example, intraseasonal and interannual

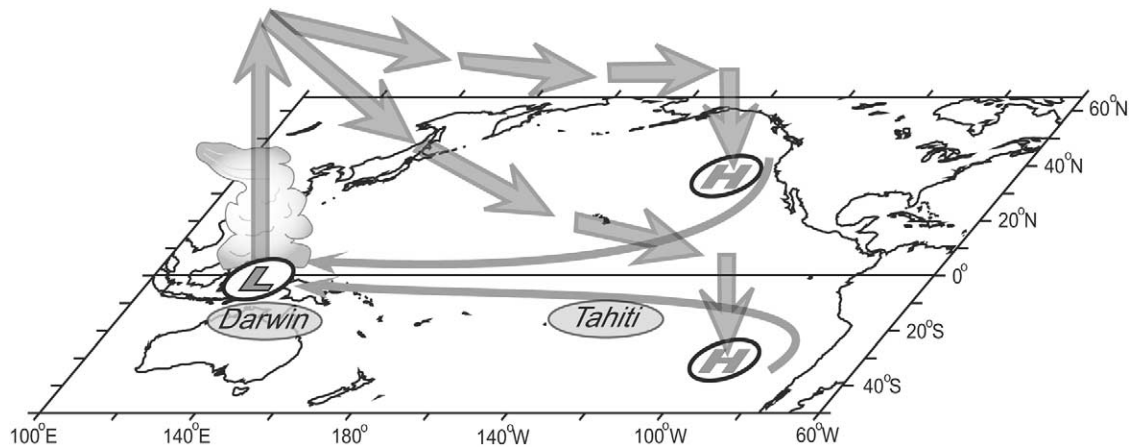


Fig. 1. A schematic illustration of the mean H–W circulation in the Pacific region. Trade winds in the lower troposphere transport air from the NPH and SPH into an area of low SLP in the western tropical Pacific-southeast Asian region. Air rises in tropical convective systems and then flows poleward and eastward as upper tropospheric winds. It then descends over the NPH and SPH. The meridional component of the H–W circulation is the Hadley circulation, and the zonal component is the Walker circulation. Through the H–W circulation, the northeast Pacific is linked to remote regions.

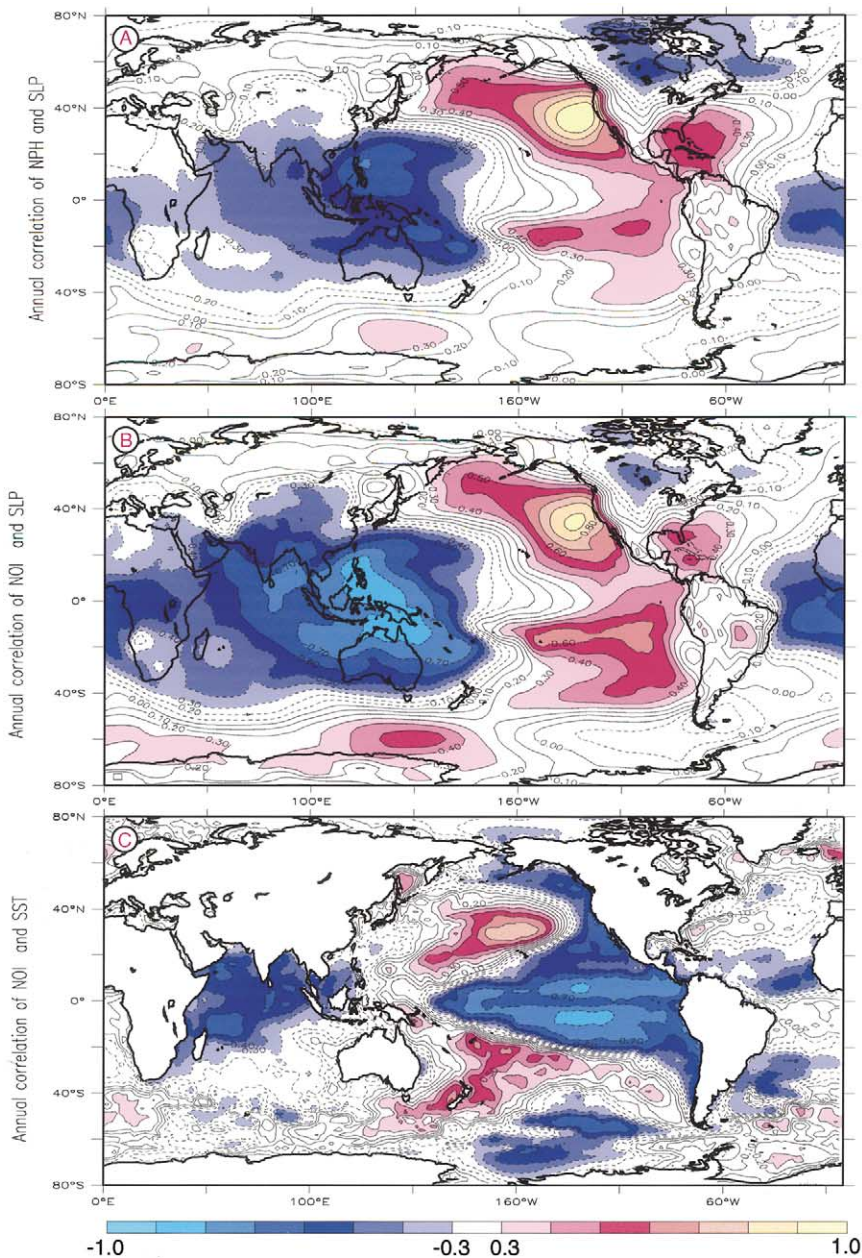


Fig. 2. (a) Correlation of annual mean SLP at the NPH (35°N, 130°W) with SLP globally. The two regions of positive correlation (yellow–red) in the northeast and southeast Pacific, and the large region of negative correlation (blue) in the western tropical Pacific show that interannual changes in the NPH are strongly coupled with variations in the H–W circulation (cf. Fig. 1). (b) Correlation of annual NOI with annual SLP globally. Yellow–red (blue) shades denote positively (negatively) correlated SLP and NOI. (c) Correlation of annual NOI with annual SST globally. Yellow–red (blue) shades denote positively (negatively) correlated SST and NOI. Period of data used in correlations is 1950–1999. Contour interval is 0.1. Significant correlations ( $|r| > 0.3$ ) are shaded. Figures based on data provided by the NOAA-CIRES CDC, Boulder, Colorado from their Web site at <http://www.cdc.noaa.gov/>.

changes in east Asia and the tropical Pacific (Horel & Wallace, 1981; Knutson & Weickmann, 1987; Nitta, 1987). The NEP is involved in and influenced by a wide range of large-scale climate changes (e.g. EN/LN events, variations of the Asian monsoon) through fluctuations in the north Pacific H-W circulation (Bjerknes, 1966, 1969; Ford, 2000; Schwing et al., 2002). These are teleconnected to and reflected in the NEP as changes in SLP, surface winds, and other atmospheric and oceanic variables.

To identify the areas that have the most impact on climate variations in the NEP, SLP at the center of the NPH's climatological mean position (35°N, 135°W) was correlated with SLP globally (Fig. 2a). As expected, NPH SLP is positively correlated with SLP in most of the NEP. There is an almost equally strong but negative correlation with SLP covering most of the tropical Indian Ocean, southeast Asia, and western tropical Pacific. An area of positive correlation occurs in the tropical and subtropical southeast Pacific. The positively correlated regions in the northeast and southeast Pacific, along with the area of negative correlation in the western tropical Pacific, reflect mass transfer and pressure variations in the Pacific H-W circulation (Fig. 1).

Fig. 2a indicates that climate variations in the NEP are linked to those in a wide range of remote locations, especially the western tropical Pacific. Correlating SLP in the SPH with SLP globally yields a similar pattern (not shown; cf. Trenberth & Shea, 1987). These initial findings led us to develop a climate index for the north Pacific-North American region based on SLP in the NEP and the western tropical Pacific. This index, the Northern Oscillation Index (NOI), incorporates both tropical and extratropical atmospheric variations, which combine to impact much of the Northern Hemisphere. Thus the NOI has the potential to capture a number of climate variations and their effects on the NEP, and the broader north Pacific-North American region.

In this report, we describe how the NOI is derived, compare it to the SOI, and discuss its value in analyzing climate variations, especially in the NEP. We highlight the principal features of the NOI time series, relate it to global atmospheric and oceanic parameters, and compare this index to representative physical and biological time series from the NEP. Our objectives are to demonstrate that variability in the north Pacific (H-W) circulation, as measured by the NOI, is a useful indicator of: (1) climate fluctuations in the NEP; (2) global climate teleconnections to the NEP; and (3) mechanisms linking the physical environment to marine resource variability in the NEP.

### 1.1. Why a new index?

There are many climate indices that help explain climate variations in the north Pacific-North American region. The SOI in particular is well correlated with a wide range of extratropical climate variations, including many in the NEP (Peixoto & Oort, 1992; Philander, 1990; Pulwarty & Redmond, 1997; Redmond & Koch, 1991). So why is a new climate index for the NEP needed?

The SOI is a good measure of tropical Pacific climate variations, especially EN/LN variations (Chen, 1982; Trenberth & Shea, 1987). But since it is based entirely in the tropics, the SOI has only a statistical relationship with extratropical climate variations. Tropical SLP variations described by the SOI are linked indirectly to extratropical climate fluctuations via the Pacific H-W circulation (Fig. 2; also see Bjerknes, 1966, 1969; Philander, 1990). The absence of a physical link between the SOI and the extratropics makes it difficult to identify the mechanisms of extratropical climate variations based on the SOI. Also, on some occasions, extratropical anomaly patterns are inconsistent with those in the tropics, and the magnitude and/or sign of the SOI. For example, north Pacific anomalies during the 1995–1997 LN differed significantly from those typically seen during LN events (Schwing et al., 2002).

A number of extratropically based indices give relatively good descriptions of atmospheric variations that occur primarily within the extratropics (e.g. NPI, NAO, East Pacific Index, Arctic Oscillation). However these indices are only indirectly linked to the tropics, a major source of global climate variability (Peixoto &

Oort, 1992). In particular, they are limited in their ability to represent transports of mass, momentum, and energy between the tropics and extratropics.

In analyzing extratropical climate variations and their links to the tropics, it makes sense to consider an index that captures the major tropical variations that affect the extratropics (e.g. EN/LN variations represented by the SOI), but also has a clear physical connection to the extratropical region being analyzed. Because the NOI is based on the difference in SLPAs in the NEP and western tropical Pacific, it gives a good indication of both tropical and extratropical variations, and also the meridional and zonal teleconnections that link these regions (Figs. 1 and 2a). The NOI is partially based in the NEP, so it includes information about atmospheric factors that directly impact the NEP (Miller et al., 1994; Parrish et al., 2000; Schwing et al., 2002). Because it is partially based in the western tropical Pacific, it also contains information about a number of major climate variations with global impacts, including EN/LN events, Madden-Julian oscillations, and intraseasonal to decadal variations of the Asian–Australian monsoon system (Ford, 2000; Knutson & Weickmann, 1987; Meehl, 1997; Nitta, 1987). Thus the NOI may provide a relatively direct means for identifying the regional and remote processes that drive climate change in the NEP.

### 1.2. The 1997–1998 El Niño event

The widespread impacts of variations in the Pacific H-W circulation are especially clear during EN/LN events (Bjerknes, 1966, 1969; Gill, 1982; Philander, 1990). Many major tropical and extratropical atmospheric and oceanic anomaly patterns are associated with EN/LN, and correlated with the SOI. The climate anomalies that occurred during the onset of a major EN in 1997–1998 illustrate the potential value of the NOI in identifying the impacts of atmospheric anomalies on the NEP.

In February 1997, an anticyclonic (clockwise) surface wind stress anomaly associated with higher than normal NPH SLP covered the NEP (Fig. 3a). By May 1997, a cyclonic surface wind stress anomaly indicative of weaker than normal SLP had developed over this region (Fig. 3b). The centers of the anomalous February anticyclone and May cyclone were near the annual mean position of the NPH (the open circle at 35°N, 130°W). In both February and May 1997, the trade wind anomalies over the southeast Pacific were similar to, but weaker than, the NEP anomalies.

February marked the end of the 1995–1997 LN (Schwing et al., 2002). May wind anomalies, in the early stage of the 1997–1998 EN, were similar to those in the early stages of past EN events but were much stronger (Murphree and Schwing, personal communication). The impressive magnitude of the north Pacific anomalies during these times, and the rapid transition from one anomaly pattern to the other, indicates a strong teleconnection between the tropics and extratropics. Upper tropospheric circulation and surface stress anomaly patterns were equivalent barotropic (i.e. the anomalies were qualitatively similar) at these times, and may have been related to the unusual upper ocean anomaly patterns observed in early 1997 (Schwing et al., 2002).

The anomaly fields shown in Fig. 3a and b are representative of those seen during much of the 1995–1997 LN and 1997–1998 EN, respectively, and are linked to the evolution of EN conditions in the tropical Pacific (Schwing et al., 2002). These wind stress anomalies are also representative of those seen during the onset of previous EN/LN events (Murphree and Schwing, personal communication) and during decadal climate regimes (Parrish et al., 2000). The February and May 1997 patterns also illustrate anomaly patterns when the NOI is positive and negative, respectively, as discussed in sections 3.2 and 3.3. These wind patterns suggest that an index based on SLPs in the NPH and western tropical Pacific would be a good indicator of the regional and remote atmospheric mechanisms that together influence oceanic anomalies in the NEP.

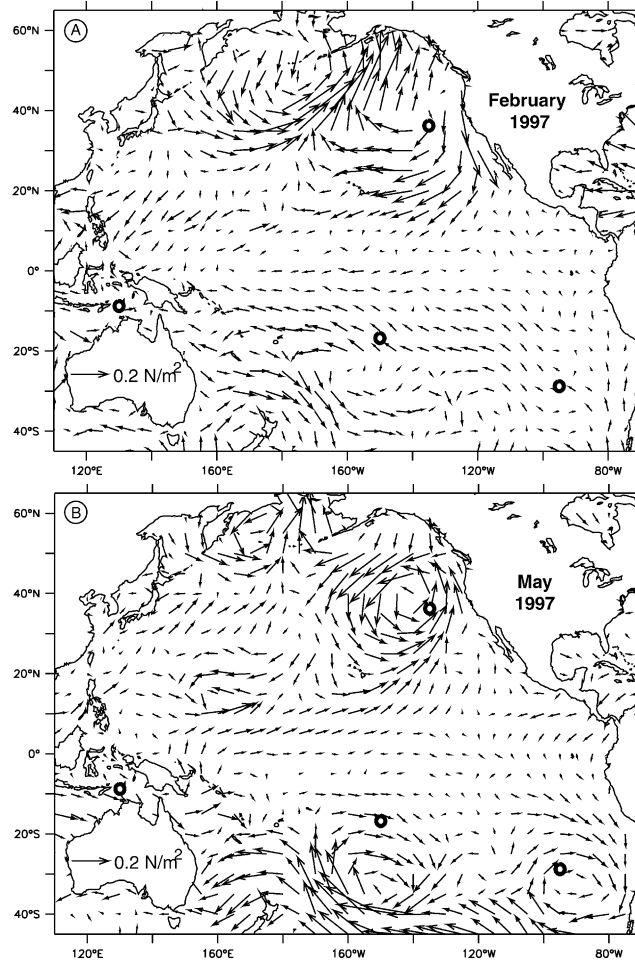


Fig. 3. Monthly mean wind stress anomalies for (a) February 1997 and (b) May 1997. Open circles mark the annual mean positions of the locations used in the computation of the NOI, SOI\*, and SOI (Eq. (1)); the NPH (35°N, 130°W), SPH (30°S, 95°W), Darwin (10°S, 130°E), and Tahiti (18°S, 150°W). The annual mean NPH position was near the center of the major northeast Pacific wind stress anomaly patterns for both months. Scaling vector shown in lower left.

## 2. Data and methods

Our primary data sets were the global atmospheric and oceanic reanalysis fields for 1948–2001 from the National Centers for Environmental Prediction (NCEP) described by Kalnay et al. (1996). These fields were obtained from, and partially processed at, the NOAA-CIRES Climate Diagnostics Center (CDC) web site (<http://www.cdc.noaa.gov/>). The main fields were gridded (roughly  $2.5^\circ \times 2.5^\circ$ ) monthly anomaly fields of SLP, SST, and surface wind velocity (used to calculate surface wind stress anomalies). The base period for computing the NCEP reanalysis field anomalies is 1968–1996. Correlation maps were developed using the CDC web site.

Subsurface (150 m) temperature anomaly time series were developed for two west coast areas, southern California (32–33°N, 117–118°W) and Washington (47–49°N, 126–128°W), from the World Ocean Database 1998 (WOA98) data base (Levitus et al., 1998). These temperature series were detrended after removing

the monthly climatologies. The base period for computing these anomalies was 1951–1993. The comparisons made here involve a variety of data sets and types with different base periods. Our results and relationships are not significantly altered by changing the base period. We use the climatologies created by the groups that have provided the individual data sets.

We computed the NOI from the NCEP reanalysis monthly SLPA time series for January 1948–May 2001 at the climatological mean position of the center of the NPH (35°N, 130°W) minus the SLPA series near Darwin, Australia (10°S, 130°E). We also calculated an analogous Southern Oscillation Index (SOI\*) from the SLPA at the climatological annual mean center of the SPH (30°S, 95°W) minus Darwin SLPA. We compared these to the most commonly used SOI, one based on Tahiti SLPA (18°S, 150°W) minus Darwin SLPA (cf. Chelliah, 1990). For these indices, the SLPAs were computed by subtracting the 1948–97 climatologies from the monthly averaged SLP observations. These anomalies were then used to construct the following series:

$$\text{NOI} = \text{SLPA}(\text{NPH}) - \text{SLPA}(\text{Darwin}) \quad (1a)$$

$$\text{SOI*} = \text{SLPA}(\text{SPH}) - \text{SLPA}(\text{Darwin}) \quad (1b)$$

$$\text{SOI} = \text{SLPA}(\text{Tahiti}) - \text{SLPA}(\text{Darwin}) \quad (1c)$$

where  $\text{SLPA}() = \text{actual monthly SLP}() - \text{climatological monthly SLP}()$ .

Each of these indices is calculated so that LN (EN) events are represented by extended periods when the indices are positive (negative).

We compared four normalized and non-normalized versions of these three indices.

1. The series were normalized twice. First, the SLPA time series were normalized by their standard deviation. Then the indices, computed as the difference of the normalized series, were normalized by the standard deviation of the difference of the anomalies (the common derivation of the SOI used by Chelliah, 1990).
2. The SLPA series were normalized by the standard deviation of the series, then the indices were computed as the difference of the normalized series.
3. The SLPA series were normalized by the monthly standard deviation, then the indices were computed as the difference of the normalized series.
4. The indices were computed from the SLPA series with no normalizing of the SLP or indices.

We selected the non-normalized form (Version 4) for this study for several reasons. First, the non-normalized versions more clearly describe the relative contributions of the individual SLP series and their impacts on surface wind (e.g. trade wind) anomalies. Second, subtle shifts in the timing of SLP anomalies, which can reveal details on the evolution of climate anomalies, are better represented by the non-normalized indices. Finally, the major temporal variations of the normalized and non-normalized indices (Eq. (1a)–(1c)) are very similar. So the simplest version, based on the non-normalized anomalies, was used to generate the indices described here. The resulting indices were then smoothed with a five-month running average. The non-normalized NOI, SOI, and SOI\* described here are available online at: <http://www.pfeg.noaa.gov>.

### 3. Results

#### 3.1. Comparison of index time series

The five-month smoothed time series of the NOI, SOI, and SOI\* are shown in Fig. 4. The dominant variability in these series is on the interannual scale generally identified with EN/LN events. Large positive

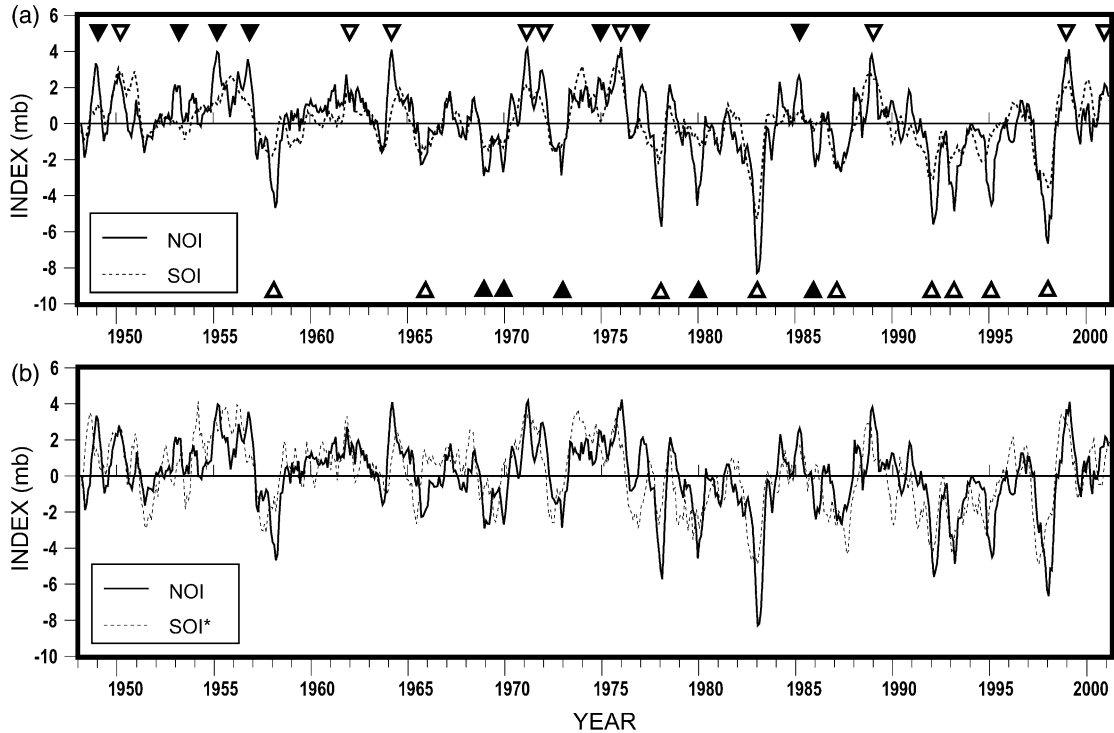


Fig. 4. Monthly time series for January 1948–May 2001 of (a) the NOI (solid grey line) and the SOI (dashed line); and (b) the NOI (solid grey line) and an alternate SOI\* (dashed line). The 1948–1997 monthly mean SLPs at each location were removed prior to computing the three indices, per Eq. (1). The series were smoothed with a five-month running filter. Moderate/strong positive (negative) events in the NOI are identified by downward (upward) pointing triangles. Open (solid) triangles indicate events that are (are not) classified by the SOI as moderate to strong events. Time periods dominated by negative values of the NOI are shaded.

(negative) index values are usually associated with LN (EN) events and cool (warm) upper ocean temperature anomalies in the NEP, particularly along the North American west coast (Fig. 2c). A 53-year (1948–2001) chronology of the magnitude of the positive and negative events for the three indices is given in Table 1. The dates of moderate/strong events in the NOI and SOI series are shown in Table 2.

The similarity of the three series on interannual scales reflects the tendency of the NPH, SPH, and Tahiti to vary together, and out-of-phase with the low near Indonesia (cf. Fig. 2a). Darwin and the NPH are both important contributors to most major interannual events in the NOI (Fig. 5; e.g. 1971–1972, 1982–1983, 1997–1998). However, there are other events when the NOI values are almost exclusively the result of the NPH anomaly (e.g. 1957–1958, 1985–1986). NPH SLP has a higher amplitude than Darwin and is more variable on interannual and intra-annual scales, particularly during winter. The NOI has a strong positive correlation with the NPH series ( $r = 0.92$ ) and a weaker negative correlation with Darwin SLP ( $r = -0.77$ ). The correlation between the NPH and Darwin is  $r = -0.45$ .

The NOI and SOI are highly correlated ( $r = 0.77$ ) and have a similar overall appearance, but feature differences that may reflect distinct climate patterns and a different set of individual climate events. The NOI has larger amplitude and is more variable (NOI s.d. = 1.92mb; SOI s.d. = 1.38mb). While the SOI is more often associated with EN events, through its negative anomalies, positive (21) and negative (19) events occurred nearly equally (Fig. 6, Table 3). In contrast, the NOI had nearly twice as many positive (32) as negative (17) events. The NOI identified 16 moderate/strong positive events and 14 moderate/strong

Table 1

Rank of positive and negative events in NOI, SOI, and SOI\*, by year (defined as July year( $n-1$ )-June year( $n$ )). Intensity was determined objectively by comparing maxima/minima values in a year to the standard deviation (s.d.) of each monthly index series. Periods with index values that are: within 0.5 s.d. of the mean are classed as neutral periods (denoted by 0); 0.5–1 s.d. from the mean are classed as weak ( $\pm 1$ ) events; 1.0–2.0 s.d. are moderate ( $\pm 2$ ); 2.0–3.0 s.d. are strong ( $\pm 3$ ); > 3.0s.d. are very strong ( $\pm 4$ ). \*\*/## denotes the strongest positive/negative event in each series; \*/# denotes the five strongest positive/negative events in each series

	NOI	SOI	SOI*		NOI	SOI	SOI*
1948–1949	2	1	2	1975–1976	3*	3**	2
1949–1950	2	3*	2	1976–1977	2	0	-2
1950–1951	1	3*	2	1977–1978	-3#	-2	-2
1951–1952	-1	-1	-2	1978–1979	1	-1	-2
1952–1953	2	0	1	1979–1980	-3	-1	-2
1953–1954	1	1	3**	1980–1981	-1	-1	-1
1954–1955	3*	1	2	1981–1982	0	0	0
1955–1956	1	2	3*	1982–1983	-4###	-4###	-3###
1956–1957	2	1	1	1983–1984	1	0	0
1957–1958	-3#	-2	-2	1984–1985	2	0	1
1958–1959	0	-1	0	1985–1986	-2	0	0
1959–1960	1	0	0	1986–1987	-2	-2#	-2#
1960–1961	1	0	0	1987–1988	1	0	0
1961–1962	2	2	2	1988–1989	2	2*	2
1962–1963	-1	-1	0	1989–1990	1	-1	-2
1963–1964	3*	2	2	1990–1991	1	0	-2
1964–1965	1	0	-2	1991–1992	-3#	-3#	-3#
1965–1966	-2	-2	1	1992–1993	-3	-2#	-3#
1966–1967	1	1	1	1993–1994	0	0	0
1967–1968	1	1	2	1994–1995	-3	-2	-2
1968–1969	-2	-1	-2	1995–1996	0	1	2
1969–1970	-2	-1	0	1996–1997	1	1	1
1970–1971	3*	2	2*	1997–1998	-4#	-3#	-3#
1971–1972	2	2	-2	1998–1999	3**	2	2*
1972–1973	-2	-1	-2	1999–2000	1	2	2
1973–1974	1	3*	2*	2000–2001	2	2	2
1974–1975	2	0	2				

negative events since 1948 (Figs. 4a and 6, Table 2). Thus positive events were more likely than negative events to be categorized as weak. A biennial oscillation between EN and LN states is not evident in these indices. Just 8% (25%) of the past 53 years are classified by the NOI (SOI) as neutral (neither positive nor negative; Table 3).

Only nine (56%) positive and nine (64%) negative moderate/strong NOI events (open triangles in Fig. 4a) are classified likewise by the SOI (Table 3). The very strong 1957–1958 EN is an example of an important difference between the NOI and the SOI. This event had major impacts on the NEP (cf. Sette & Isaacs, 1960) and helped lead to the realization that EN/LN events have global impacts. It is clearly indicated by the NOI but is only a minor feature in the SOI. Another notable difference occurred in 1984–1985, when the NOI was strongly positive but the SOI was neutral. At that time, strong atmospheric and oceanic anomalies like those typical of LN occurred in the NEP, while tropical Pacific anomalies were weak. Even when the sign and magnitude of these indices agreed, the timing of peaks in the events often differed by several months (e.g. 1955–1956, 1994–1995).

Negative and positive events in the indices have often occurred in multi-year clusters, suggesting decadal-scale regimes. The well-documented decadal climate shift that occurred in 1977 (cf. Ebbesmeyer et al., 1991; Nitta & Yamada, 1989; Trenberth, 1990; Trenberth & Hurrell, 1994) is seen in the NOI as a change

Table 2

List of moderate, strong, and very strong positive and negative events in the NOI and/or the SOI. Rank of Cold ( $> 0$ ) and Warm ( $< 0$ ) events in NOI and SOI, by year. Intensity was determined objectively by comparing maxima/minima values in a year to the standard deviation (s.d.) of each monthly index series. Periods with index values that are: within 0.5 s.d. of the mean are classed as neutral periods (denoted by 0); 0.5–1 s.d. from the mean are classed as weak ( $\pm 1$ ) events; 1.0–2.0 s.d. are moderate ( $\pm 2$ ); 2.0–3.0 s.d. are strong ( $\pm 3$ );  $> 3.0$  s.d. are very strong ( $\pm 4$ ). \*\*/### denotes the strongest positive/negative event in each series; \*/# denotes the five strongest positive/negative events in series. Total refers to number of moderate/strong events for each index

	Positive events		Negative events		
	NOI	SOI	NOI	SOI	
1948–1949	2	1	1957–1958	–3#	–2
1949–1950	2	3*	1965–1966	–2	–2
1950–1951	1	3*	1968–1969	–2	–1
1952–1953	2	0	1969–1970	–2	–1
1954–1955	3*	1	1972–1973	–2	–1
1955–1956	1	2	1977–1978	–3#	–2
1956–1957	2	1	1979–1980	–3	–1
1961–1962	2	2	1982–1983	–4###	–4###
1963–1964	3*	2	1985–1986	–2	0
1970–1971	3*	2*	1986–1987	–2	–2#
1971–1972	2	2	1991–1992	–3#	–3#
1973–1974	1	3*	1992–1993	–3	–2#
1974–1975	2	0	1994–1995	–3	–2
1975–1976	3*	3**	1997–1998	–4#	–3#
1976–1977	2	0			
1984–1985	2	0	Total	14	9
1988–1989	2	2			
1998–1999	3**	2			
1999–2000	1	2			
2000–2001	2	2			
Total	16	13			

from predominantly positive to negative values (Fig. 4). Other decadal shifts are evident. Following an extended period dominated by positive values, a brief negative period occurred in 1965–1970. A seven-year sequence of moderate to strong positive events began in 1970. Strong negative events dominated after 1977, culminating in the strongest event in the record, in conjunction with the 1982–1983 EN. From 1984 to 1991, the NOI was biased toward positive values. The period after 1991 was dominated by moderate to strong negative events, until mainly positive values returned in 1998. Thus the NOI indicates substantial shifts in climate occurred in 1965, 1970, 1977, 1984, 1991, and 1998, a roughly 14-year cycle. The atmospheric and oceanic signals associated with these decadal periods of positive and negative NOI are described in section 3.3.

### 3.2. Global correlation maps

Maps of the correlation of the NOI with SLP and SST globally are shown in Fig. 2b and c, respectively. The NOI is positively correlated with SLP over the northeast and southeast Pacific (yellow-red areas in Fig. 2b) and negatively correlated with SLP over the western tropical Pacific and Indian Ocean (blue areas). These patterns illustrate that the north and south Pacific components of the H-W circulation tend to vary together on interannual time scales, and are related to the mechanisms by which upper ocean anomalies

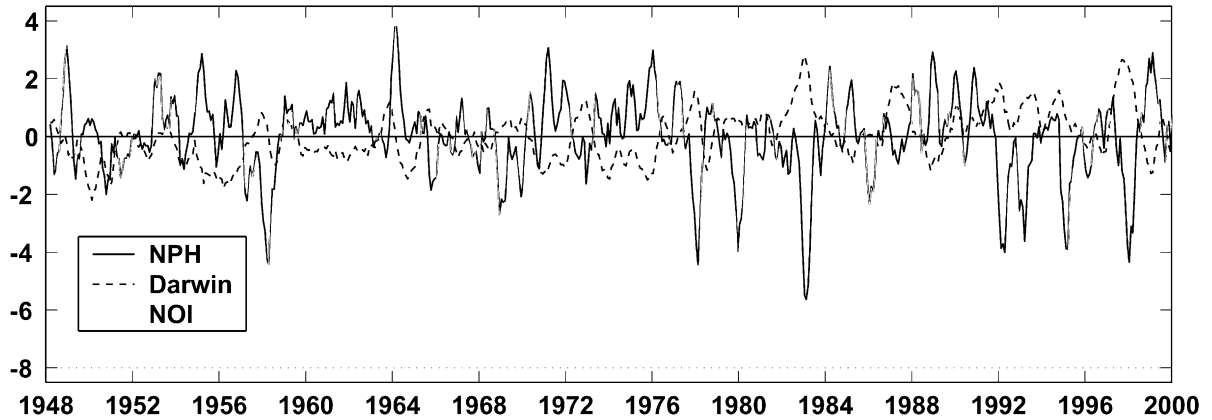


Fig. 5. Monthly time series of NOI (solid grey line), and NPH (solid black line) and Darwin (dashed line) SLPA, for 1948–2000. The 1948–1997 monthly mean SLPs at each location were removed prior to computing the three indices. The series have been smoothed with a five-month running filter.

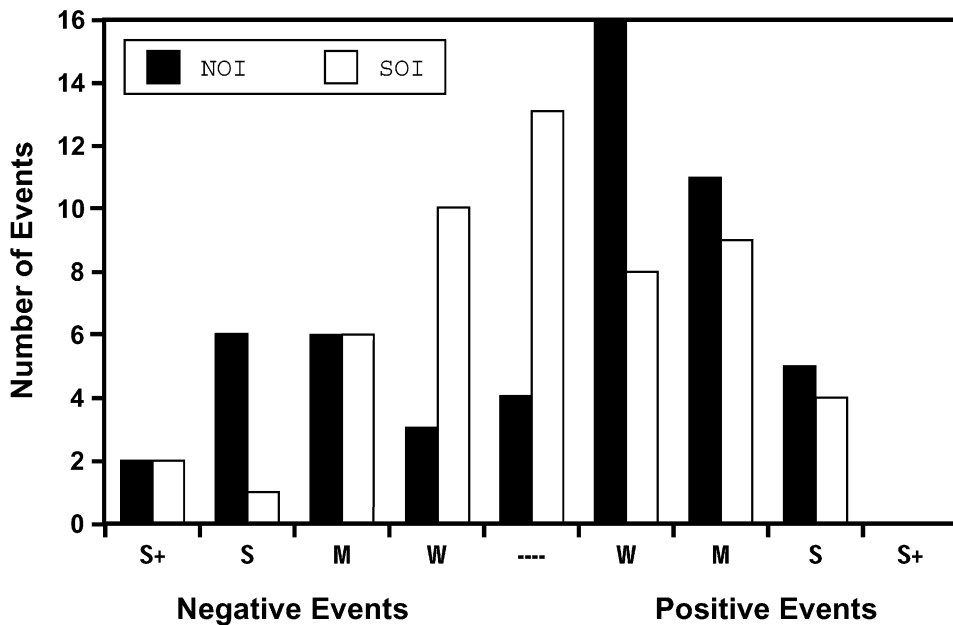


Fig. 6. The number of positive and negative events, by intensity, for NOI and SOI, based on time series in Fig. 4. Intensity was determined objectively by comparing maxima/minima values in a year to the standard deviation (s.d.) of each monthly index series. Periods with index values that are within 0.5 s.d. of the mean are classed as neutral periods (denoted by--); 0.5–1 s.d. from the mean are classed as weak (W) events, 1.0–2.0 s.d. are moderate (M), 2.0–3.0 s.d. are strong (S), > 3.0s.d. are very strong (S+).

develop in the tropical and extratropical Pacific. The SLP correlations (Fig. 2a and b) indicate shifts in atmospheric mass between the extratropical eastern Pacific and the southeast Asian-Australian region. These shifts correspond to a stronger H-W circulation when the NOI and SOI are positive, when SLP is low near Indonesia and high in the NPH and SPH, and vice versa (cf. Fig. 2). The alternating low–high–low–high

Table 3

Number of positive and negative events in the NOI and SOI by intensity, for 1947–1948 through 2000–2001 ( $n = 53$ ). Intensity was determined objectively by comparing maxima/minima values in a year to the standard deviation (s.d.) of each monthly index series. Table 1 explains the classification system. Events designated in Tables 1 and 2 as weak, moderate, strong, and very strong are designated here as W, M, S, and S+, respectively. Neutral periods are designated here with a dash (-). Horizontal and vertical sets of values outside matrix denote total number of occurrences of each type of event in the NOI and SOI, respectively. There were 32 positive and 17 negative NOI events, and 21 positive and 19 negative SOI events. Values in matrix denote number of each type of event identified in each index. If series corresponded perfectly, all values would lie on diagonal of matrix. Bold numbers refer to moderate-strong events. The NOI identifies 16 positive and 14 negative examples of moderate-strong events, while the SOI identifies 13 positive and 9 negative. Italicized numbers refer to neutral periods. The NOI identified 4 neutral periods, while the SOI identified 13

		Negative					Positive				
		S+	S	M	W	-	W	M	S	S+	
	SOI	NOI	<b>2</b>	<b>6</b>	<b>6</b>	3	4	16	<b>11</b>	5	<b>0</b>
Neg.S+	<b>1</b>	<b>1</b>									
S	<b>2</b>	<b>1</b>	<b>1</b>								
M	<b>6</b>		<b>4</b>	2							
W	10		1	3	3	<i>1</i>	2				
-	<i>13</i>			<i>1</i>		<i>2</i>	6	4			
Pos.W	8					<i>1</i>	4	2	1		
M	<b>9</b>						2	<b>4</b>	<b>3</b>		
S	<b>4</b>						2	<b>1</b>	<b>1</b>		
S+	<b>0</b>										

SLP correlation patterns in the northern and southern hemispheres (Fig. 2a and b; e.g. southeast Asia–north Pacific–North America–north Atlantic) reflect atmospheric wave trains linking the tropics and extratropics and, in particular, linking the NPH and SPH to the tropical Pacific and the southeast Asian–Australian region (Ford, 2000; Nitta, 1987; Reynolds, Gelaro, & Murphree, 1996; Schwing et al., 2002).

The NOI is positively correlated with SSTs in the central north and south Pacific (yellow-red areas in Fig. 2c) and negatively correlated along the west coast of the Americas and in the eastern tropical Pacific and Indian Ocean (blue areas). The typical pattern of negative and positive SLP and SST anomalies during LN (EN) is similar (opposite) to the pattern of positive and negative correlations in Fig. 2b and c (Schwing et al., 2002). This confirms that a positive (negative) NOI is typically associated with LN (EN) events.

To illustrate the seasonality of this relationship, and help identify the mechanisms that produce interannual variability to the North Pacific Ocean, we examined the correlation between the NOI and SST by season (Fig. 7). The NOI is more highly correlated with interannual SST variability in the extratropical North Pacific during the boreal winter and spring than in the boreal summer and autumn. There is also a relatively high correlation between winter and spring NOI and North Pacific SST during the subsequent four seasons (not shown).

These results may reflect seasonal variations in the strength of atmospheric anomalies represented by the NOI (especially North Pacific surface wind stress) and the relatively long memory of the ocean. The magnitude of the NOI tends to be greatest during the winter and spring (Fig. 4). These winter extremes represent strong wind anomalies in the north Pacific that can establish temperature anomalies in the upper ocean that remain for several seasons. Winter wind stress anomalies can affect the upper ocean through a variety of processes, including Ekman processes, geostrophic advection, surface heat fluxes, and mixing (c.f. section 4.2; Cayan, 1992; Miller et al., 1994; Miller & Schneider, 2000; Schwing et al., 2002). Winter ocean anomalies often persist into the summer when atmospheric anomalies tend to be weakest (Schwing et al., 2002). Thus the longer memory of the ocean compared to the atmosphere makes the simultaneous correlation of the NOI with the extratropical north Pacific SSTs weakest during summer, while the lagged

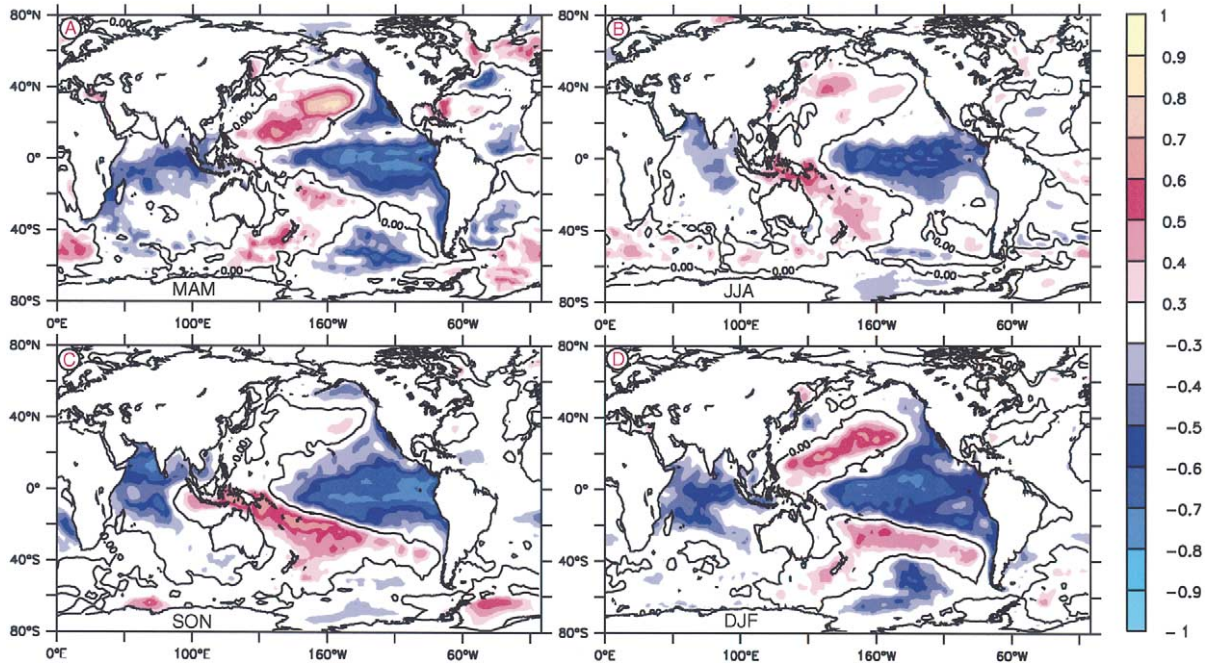


Fig. 7. Correlation of NOI with SST globally, by season; (a) spring (March–May), (b) summer (June–August), (c) fall (September–November), and (d) winter (December–February). Yellow–red (blue) shades denote significant positive (negative) correlations ( $|r| > 0.3$ ). Contour interval is 0.1. Period of data used in correlations is 1950–1999. Figures show highest correlations in winter and spring.

correlation of winter and spring NOI with subsequent SSTs is strong throughout the year. In contrast, the simultaneous correlations of the NOI with tropical Indian and Pacific SSTs are strong at all seasons (Fig. 7). This may be because of a weaker seasonal cycle in the tropics and a faster ocean internal wave response to atmospheric forcing (Gill, 1982).

The applicability of the NOI is further documented by comparing the correlation of SSTs in the NEP to the NOI, the individual NOI components (i.e. SLPA at the NPH and Darwin), and the SOI (Fig. 8). The focus here is on the boreal spring (March–May), when biological production in the North Pacific is high, but similar results were found for all seasons. Overall, NEP SST is better correlated with the NOI (Fig. 8a) than with the NPH SLPA series alone, the SOI, or Darwin SLP. The NOI is a superior indicator of SST variability in the areas where the correlation between SST and the indices is greatest, specifically in the biologically important regions of the California Current System along the North American west coast, and the North Pacific Transition Zone north of Hawaii.

### 3.3. Pacific basin anomaly fields

Composite maps showing the SLP, surface wind, and SST anomalies in the Pacific are presented for seven-year periods of predominantly positive NOI values (1970–1976, Figs. 9a and 10a) and predominantly negative NOI values (1991–1997, Figs. 9b and 10b). In 1970–1976, SLP was anomalously high over the northeast and southeast Pacific, in the vicinity of the NPH and SPH (red areas in Fig. 9a). These positive SLPA centers were associated with anomalously anticyclonic surface wind stress, including more upwelling-favorable stress in the California and Peru–Chile Current Systems and enhanced trade winds. Negative SLPA (blue areas) occurred over the southeast Asian–Australian region, and the Asian and North and

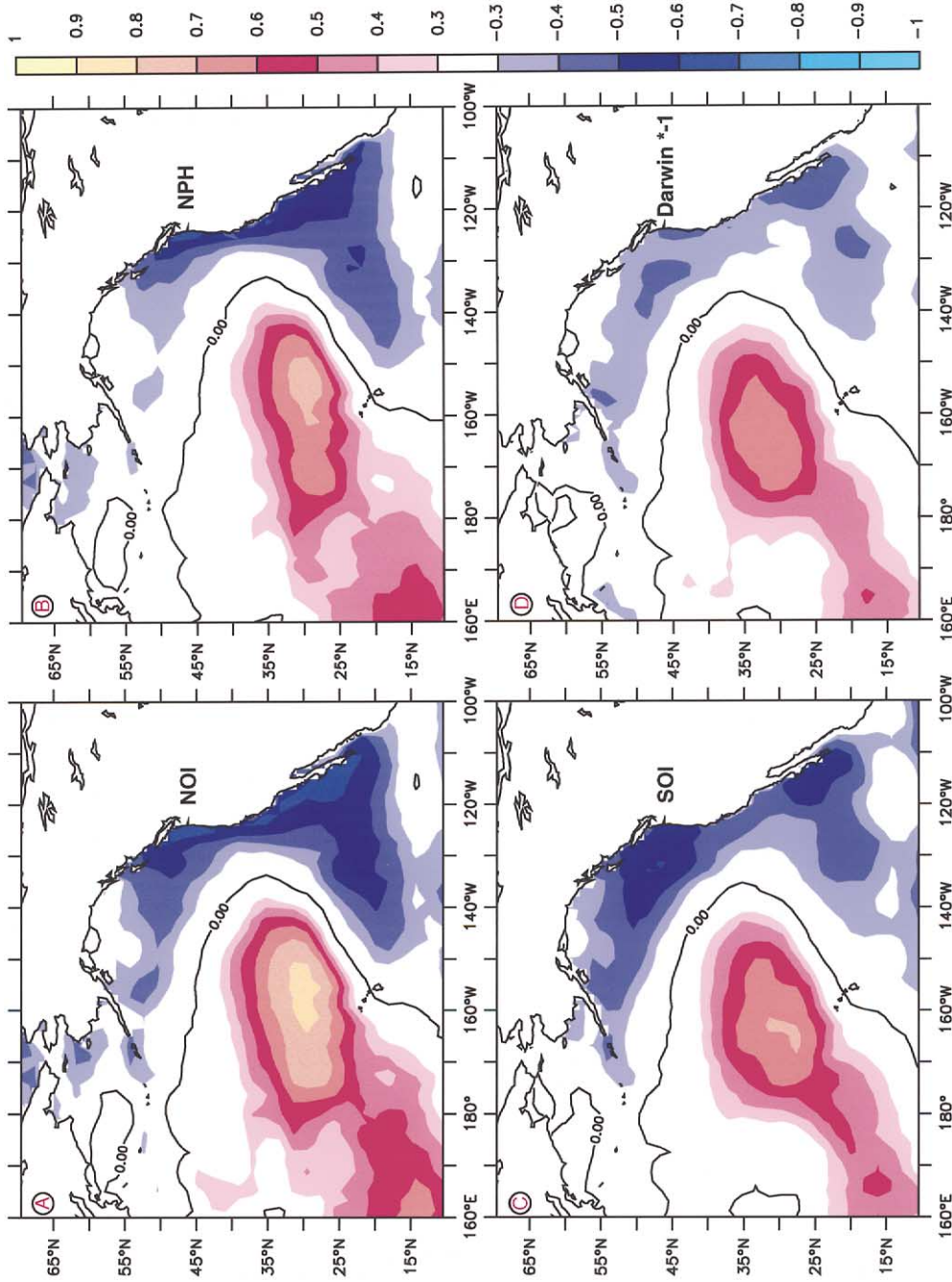


Fig. 8. Correlation of spring (March–May) SST in the northeast Pacific (NEP) with (a) NOI, (b) NPH SLPA, (c) SOI, and (d) Darwin SLPA. Yellow–red (blue) shades denote significant positive (negative) correlations ( $|r| > 0.3$ ). Contour interval is 0.1. Period of data used in correlations is 1950–1999. Figures show that NEP SST is correlated more strongly with the NOI than with the other three indices.

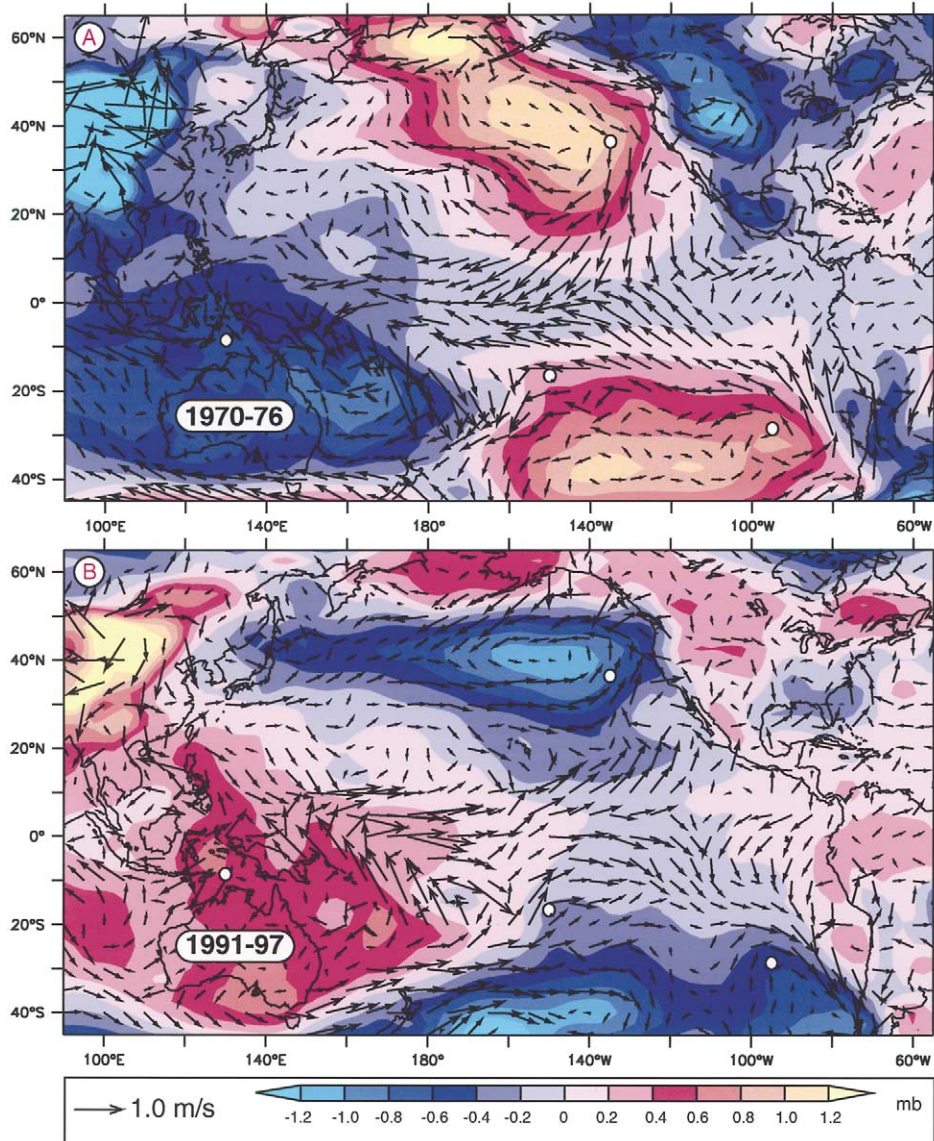


Fig. 9. Anomalies of SLP (colors) and surface wind (arrows) over the Pacific during (a) 1970–1976, a period of predominantly positive NOI values, and (b) 1991–1997, a period of predominantly negative NOI values. Yellow–red (blue) shades denote positive (negative) SLP anomalies. Contour interval is 0.2 mb; scaling arrow shown in lower left. White circles mark the climatological annual mean positions of the NPH, (35°N, 130°W), SPH (30°S, 95°W), Darwin (10°S, 130°E), and Tahiti (18°S, 150°W).

South American continents. The alternating SLP anomalies across the extratropical northern and southern hemispheres indicate an atmospheric wave train linking the tropics and extratropics. Tropical Pacific surface wind anomalies were westward and convergent in the central tropical Pacific (cf. Schwing et al., 2002). During this period of positive NOI, positive SSTAs occurred in the central north and south Pacific (red areas in Fig. 10a). Negative SSTAs (blue areas) were seen in the eastern boundary currents along the west

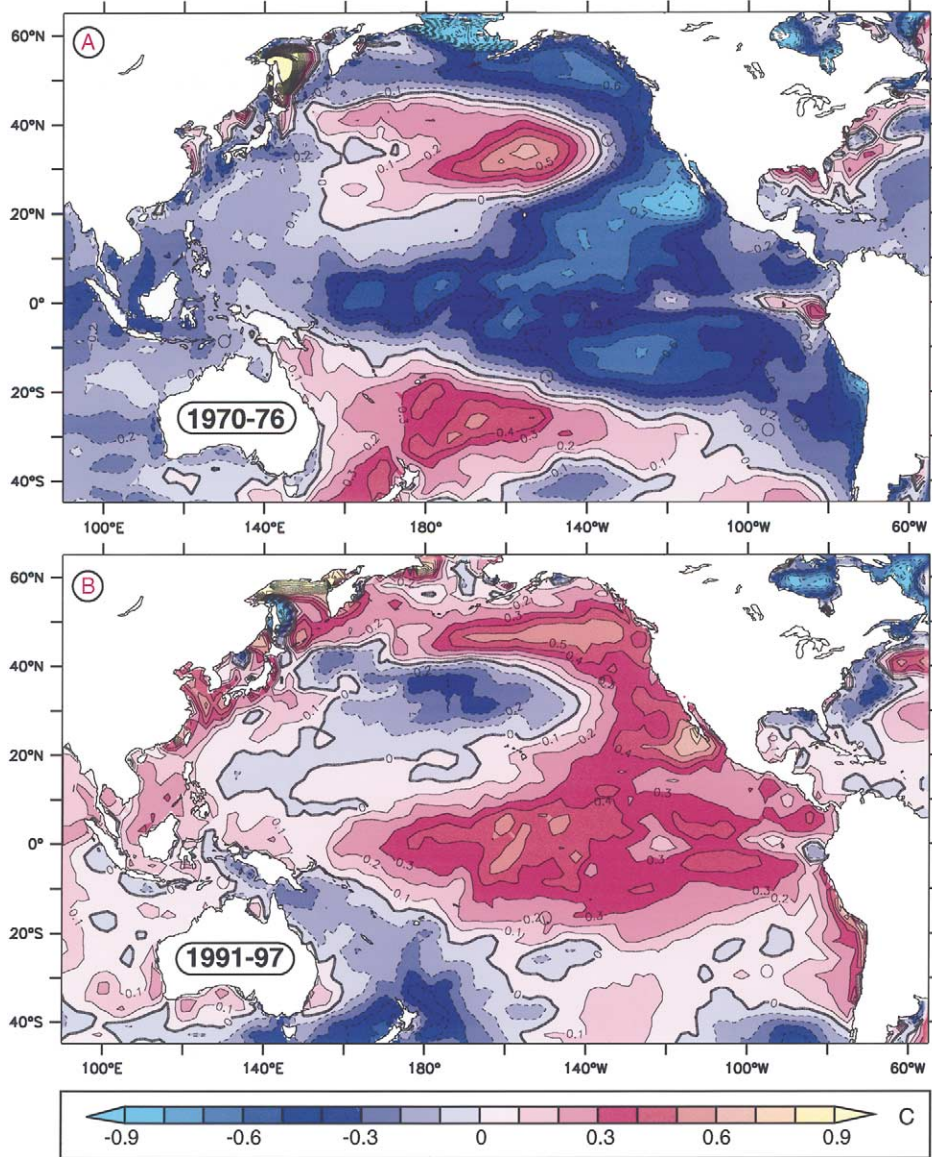


Fig. 10. SST anomalies in the Pacific during (a) 1970–1976 and (b) 1991–1997. Yellow–red (blue) shades denote positive (negative) SST anomalies. Contour interval is 0.1 °C.

coast of North and South America, the eastern tropical Pacific Ocean, and the Indian Ocean. The Pacific SSTA pattern is strikingly similar to the correlation with the NOI (Fig. 2c).

SLP and surface wind stress anomalies during the 1991–1997 period of negative NOI (Fig. 9b) are a near-mirror image to those when the NOI is positive. Important features include weaker than normal SLP over the northeast and southeast Pacific, weaker coastal upwelling favorable wind stress off North and South America, and reduced trade winds. SSTAs in this negative NOI period (Fig. 10b) are roughly opposite to those seen under positive NOI conditions. During both the positive and the negative periods, SLP, surface wind, and SST anomalies are roughly symmetric about the equator. The anomaly patterns when

the NOI is negative (positive) resemble the typical EN (LN) patterns shown by Schwing et al. (2002), who also discuss the mechanisms by which these atmospheric anomalies may produce the corresponding SSTA patterns.

### 3.4. Correlation with northeast Pacific Ocean time series

SST appears to be linked to variations in the NOI on interannual and decadal scales (Figs. 2c, 7, 9 and 10). Subsurface temperatures also fluctuate in response to atmospheric forcing through processes that affect pycnocline and mixed layer depths. This concept is supported by Fig. 11, which compares the NOI (inverted for comparison) to the detrended 150 m temperature anomaly time series off southern California and Washington. Episodes of cooler and warmer subsurface temperatures tend to correspond closely to positive and negative events in the NOI, respectively. Fluctuations in surface wind stress modify cross-shelf Ekman transport and coastal upwelling, and fluctuations in surface wind stress curl alter Ekman pumping. Both processes are closely coupled with regional SLP anomalies in the NEP, and thus are likely mechanisms for the correspondence between the NOI and temperature (cf. Miller & Schneider, 2000; Schwing et al., 2002). However remote processes that generate coastal internal waves probably contribute to this variability as well (cf. Pares-Sierra & O'Brien, 1989; Schwing et al., 2002; Strub & James, 2001).

A further example of the relative effectiveness of the NOI as an index of ocean variability is demonstrated by these series. The NOI explains more variability in the southern California ( $r = -0.65$ ) and Washington ( $r = -0.59$ ) temperature series than the NPH SLP alone ( $r = -0.56$  for both). The SOI is marginally better correlated than the NOI with southern California ( $r = -0.68$ ), but weakly correlated with Washington ( $r = -0.36$ ). Thus the NOI is similar to or better than the SOI as an index of interannual variability in the California Current System, but has a more direct physical connection to this region. The latitudinal difference in these correlations may be related to the relative importance of oceanic teleconnections. Interannual variations in the thermocline are associated with coastal-trapped waves, whose source may be fluctu-

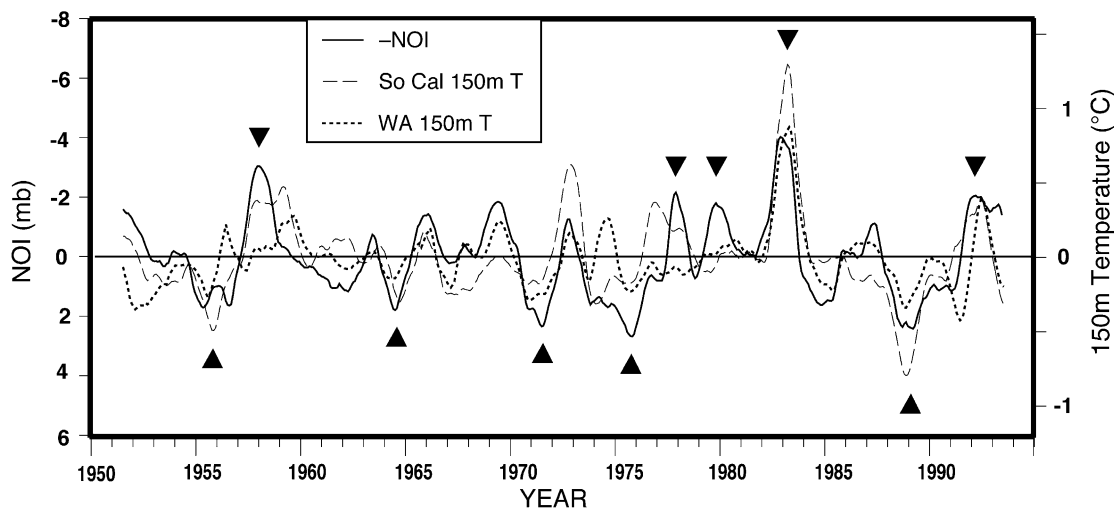


Fig. 11. The monthly NOI (solid grey line; inverted for comparison) and seasonally adjusted temperature anomalies at 150 m off southern California (32–33°N, 117–118°W; dashed line) and Washington (47–49°N, 126–128°W; dotted line) for 1951–1993. Series were detrended and smoothed with a 12-month running filter. Series trends were +0.15/decade off southern California and +0.09/decade off Washington. Correlations with the NOI are  $r = -0.65$  and  $-0.59$  for the southern California and Washington temperature series, respectively. Correlation between temperature series is  $r = 0.64$ . Downward (Upward) pointing triangles denote strong negative (positive) NOI events.

ations in equatorial wave activity (cf. Clarke & Lebedev, 1999; Strub & James, 2001) and ultimately SLP in the western tropical Pacific. Coastal-trapped waves propagate less effectively at the more northern latitudes, and hence may have less influence on temperature variability (McAlpin, 1995).

Fig. 12 shows the demeaned and detrended annual catch of western Alaska sockeye salmon and coho salmon for the Pacific Northwest for the ocean entry years 1970–1996 (after Mantua et al., 1997). The detrended series highlight an out-of-phase decadal oscillation in the Alaska and Pacific Northwest stocks between relatively high and variable returns, and low and steady returns. The detrended landings, lagged one year, are significantly correlated with the NOI (coho  $r = 0.79$ ; sockeye  $r = -0.75$ ;) and reflect the climate shifts indicated by the NOI. For example, relatively higher coho landings were associated with positive NOI values during 1970–1976 and 1984–1991, while relatively higher sockeye catches during 1978–1984 and 1993–1996 corresponded to a negative NOI. These results indicate the NOI may be a valuable index of fishery variability in the NEP.

The normalized CalCOFI 40-year time series of maximum annual macrozooplankton volume off southern California (adapted from Roemmich & McGowan, 1995) is shown in Fig. 13. This biomass series is weakly correlated with the NOI ( $r = 0.21$  after detrending). However, similarities in the interannual variations of these series suggest that changes in biomass may be explained in part by physical variability described by the NOI. All of the sharp declines in the NOI (upward-pointing triangles) are reflected as declines in macrozooplankton biomass. But biomass increases do not accompany all shifts toward positive or higher NOI values, nor are they quantitatively consistent (e.g. the increases in the NOI in 1975 and 1988). Solid (open) downward-pointing triangles denote shifts to positive NOI when biomass does (does not) rebound. Thus a negative NOI may correspond to poor conditions for zooplankton (e.g. lesser coastal upwelling), which result in population declines. But populations do not necessarily expand given the good conditions presumably associated with positive NOI. The NOI probably represents only some of the factors driving zooplankton population dynamics. Nevertheless it has been shown to be a useful index for investigating

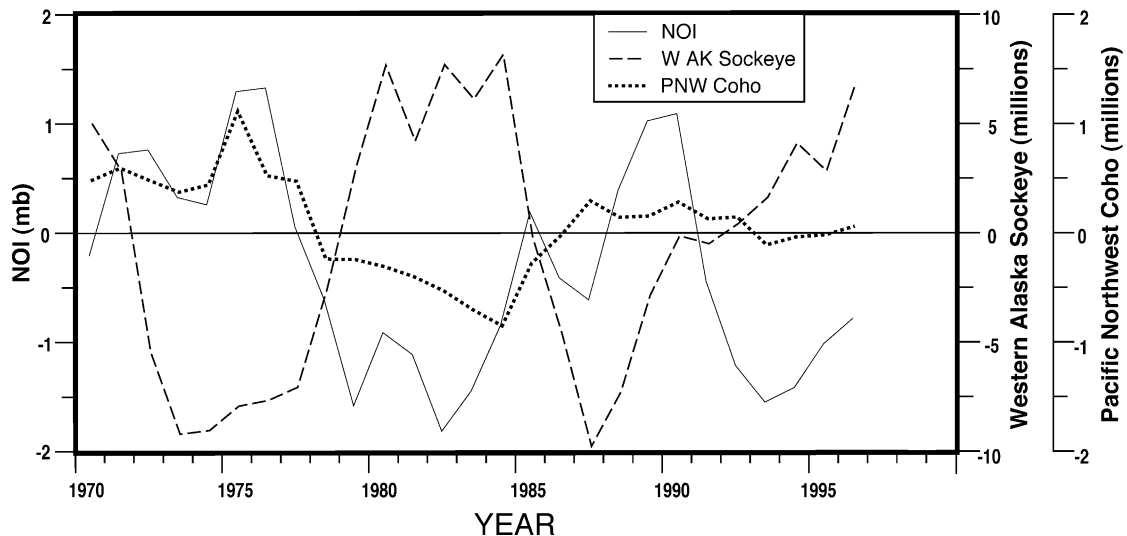


Fig. 12. The annual NOI (solid line) and the annual catch (in millions of fish) of western Alaska sockeye salmon (dashed line) and Pacific Northwest coho salmon (dotted line) for 1970–1996. Series were demeaned, detrended and smoothed with a 3-year average. The sockeye (coho) mean and trend are about 16.7 and 1.4 million fish/yr (about  $-1.5$  and  $-0.1$  million fish/yr), respectively. The correlation of the sockeye (coho) series with the NOI is  $r = -0.75$  ( $r = 0.79$ ). Correlation between salmon series is  $r = -0.69$ . Shading indicates periods dominated by relatively higher sockeye (lower coho) catch.

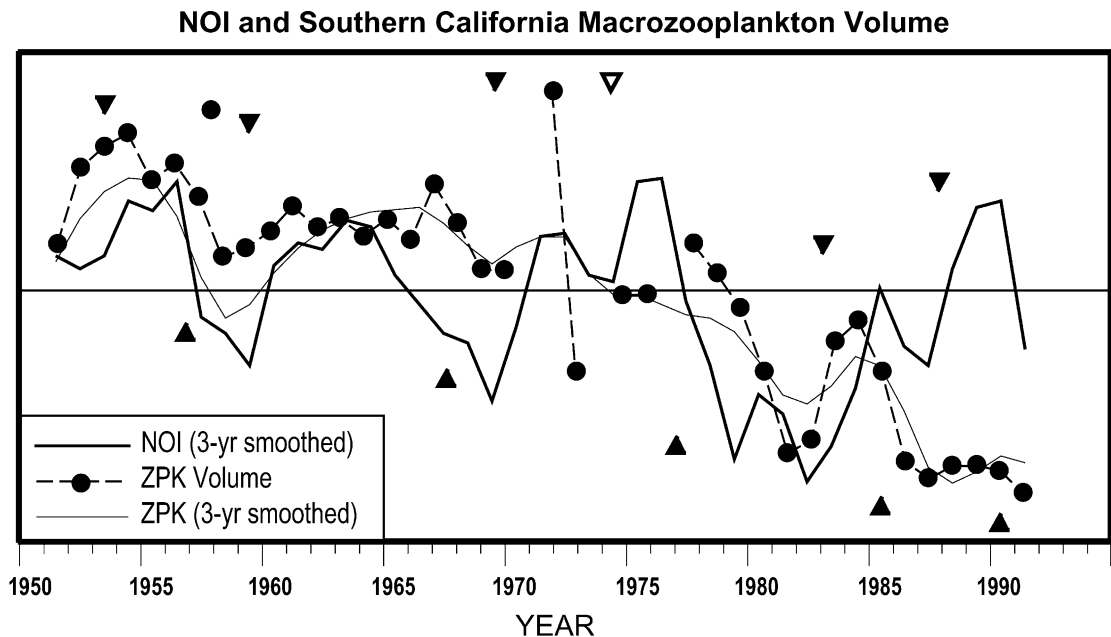


Fig. 13. Three-year smoothed NOI (solid grey line) and maximum annual macrozooplankton volume along CalCOFI Line 90 off southern California (adapted from Roemmich & McGowan, 1995) for 1951–1992. Shaded circles connected by broken lines denote volume for individual years; fine solid line is the three-year smoothed volume. The correlation between the series is  $r = 0.44$  (0.21 after both series are detrended). Shifts toward positive (negative) NOI values noted by downward (upward) pointing triangles. Solid (open) triangles denote NOI events where biomass does (does not) appear to respond to a shift in the NOI.

the relationships between climate and plankton variability off British Columbia (Mackas, Thomson, & Galbraith, 2001).

#### 4. Discussion

Many studies have shown that the SOI is well correlated with variations in north Pacific winds, SST, and many other fields (Horel & Wallace, 1981; Pulwarty & Redmond, 1997). While the NOI and SOI have a similar overall appearance, they also have important differences, which suggest that the NOI represents climatic extremes that are not well represented by the tropically based SOI. These are most likely to result from differences between the tropical and the extratropical variability on these time scales. The indices therefore reflect latitudinal variations in the forcing and response of the climate system.

Similarities between the NOI and SOI suggest the latter has been a useful indicator of climate variations in the NEP because of its links to teleconnection processes. The major differences between the NOI and SOI support the conclusion that the NOI may be a more appropriate indicator of NEP variability. Since the NOI is based in both the tropical Pacific and the NEP, it probably provides a better measure of those teleconnections. The NOI is also likely to be a more revealing monitor of climate change over the North Pacific-North American region, and a better indicator of the mechanisms that produce those changes.

#### 4.1. *El Niño, La Niña and teleconnections*

Interannual changes in the north Pacific atmosphere and ocean, which are identified by extrema in the NOI, are closely tied to tropical Pacific anomalies such as EN/LN (Mysak, 1986; Schwing et al., 2002; Wooster & Fluharty, 1985). During EN events, surface wind anomalies over the extratropical north Pacific tend to produce negative SSTAs in the central north Pacific and positive SSTAs in the NEP, initiated in large part by Ekman processes (Schwing et al., 2002). The reverse is true during LN events.

Throughout the year, wind anomalies are often part of organized and extensive tropospheric circulation anomalies that are part of Rossby wave trains initiated remotely by convective anomalies (Ford, 2000; Nitta, 1987; Schwing et al., 2002). The sources of these wave trains are the tropical Pacific, especially during boreal winter, and south and east Asia, especially during boreal late summer–winter. Since the NOI is linked to and expresses these circulation anomalies (Figs. 2b and 9), this index is a diagnostic of environmental anomalies throughout the year and from many source regions. However, it appears that winter and spring values of the NOI represent mechanisms that have the greatest and more lasting effect in the NEP (Fig. 7). The strongest and most persistent wind anomalies tend to occur from late boreal autumn through early spring, resulting in SST and other upper ocean anomalies that can last for several months to several seasons. Summer and autumn wind anomalies are generally difficult to link directly to EN or LN anomalies in the tropical Pacific. More often they are the result of atmospheric convection anomalies in the western tropical Pacific-southeast Asian region (e.g. Asian summer monsoon anomalies) (Ford, 2000; Nitta, 1987).

Atmospheric teleconnections occur not only on the interannual scale of EN/LN but also on other time scales (e.g. intraseasonal Madden-Julian oscillations and Asian monsoon fluctuations; biennial Asian monsoon fluctuations; decadal tropical Indo-Pacific variations; see Ford, 2000; Knutson & Weickmann, 1987; Meehl, 1997; Nitta, 1987; Schwing et al., 2002). Teleconnections are dynamically similar regardless of time scale (cf. Hoskins & Karoly, 1981; Murphree & Reynolds, 1995; Nitta, 1987; Reynolds et al., 1996). Thus a relatively small number of mechanisms may underlie many of the climate variations that occur in the north Pacific–North America region. Periods when strong atmospheric teleconnections to this region develop, during EN/LN for example, can reveal a great deal about how longer term climate changes of significance to ocean and ecosystem processes occur.

Oceanic teleconnections, most notably coastal-trapped waves that propagate poleward along the eastern Pacific boundary, represent another source of interannual variability. Eastward-propagating equatorial Kelvin waves are a possible source of these coastal waves (Jacobs et al., 1994; McPhaden & Yu, 1999; Schwing et al., 2002). Intraseasonal equatorial Kelvin waves, a common signal during EN events, are linked to SLP anomalies in the western tropical Pacific and anomalies in tropical and trade winds. These are incorporated in the NOI through Darwin SLP and the NPH–Darwin SLP gradient. The NOI represents regional wind anomalies in the NEP and atmospheric and oceanic teleconnections, which combine to produce much of the EN/LN signal in the extratropical Pacific.

#### 4.2. *The NOI as an index of physical and biological variability*

The NOI is significantly correlated with SST over much of the global ocean (Figs. 2c and 10) and subsurface temperature along the US west coast (Fig. 11). Major climate changes are characterized by strong and distinct anomaly patterns in SST and other upper ocean measures, particularly in the extratropical north Pacific (Deser, Alexander, & Timlin, 1996; Mantua et al., 1997; Miller et al., 1994; Miller & Schneider, 2000; Parrish et al., 2000; Schwing et al., 2002). The immediate causes of these oceanic anomalies include: (1) air–sea heat fluxes; (2) lateral Ekman transport of near-surface waters; (3) vertical transport by Ekman pumping, caused by divergence in the surface Ekman layer; (4) vertical mixing, primarily imparted by wind-induced turbulence; (5) geostrophic advection, generally the results of adjustments in horizontal pressure and temperature gradients by Ekman transport; (6) the displacement of internal structure

by low-frequency internal ocean waves; and (7) changes in upper ocean stability caused by these other processes. All of these processes are driven by atmospheric forcing, with surface wind stress being the principal forcing factor.

Process 1 is thought to be especially important in creating the basic SST response to many wind anomalies (Cayan, 1992). Through processes 2–5, these wind variations may be an important mechanism for creating upper ocean anomalies in the NEP on seasonal as well as interannual and decadal scales (Deser et al., 1996; Miller et al., 1994; Miller & Schneider, 2000; Schwing et al., 2002). For example, uniformly positive or negative upper ocean temperature and sea surface height anomalies are often found in the region marked by Vancouver Island, Hawaii, and Cabo San Lucas (Schwing et al., 2002; cf. Fig. 10). Changes in the magnitude and position of the NPH induce shifts in the strength and location of these oceanic anomalies (Knutson & Manabe, 1998; Schwing et al., 2002) through a combination of the wind-driven processes 1–5 described above.

Process 6 introduces oceanically-teleconnected climate change from as far away as the tropical Pacific (Jacobs et al., 1994; Strub & James, 2001). These variations are ultimately linked to changes in the NOI; for example, through the connection of Darwin SLP to tropical Pacific wind anomalies and the generation of equatorial Kelvin waves. Coastal oceanic anomalies extend along most of the North American west coast, and are the combined effect of the seven processes (Miller et al., 1994; Miller & Schneider, 2000; Schwing et al., 2002). Thus all of these regional and remote processes that drive SST and, more generally, upper ocean variability in the NEP have a dynamical connection with the NOI.

We have also shown two examples of the NOI as a potential index of biological variability in the NEP. The NOI, also referred to as the NOI<sub>x</sub> in some citations, has been used in recent studies as an effective environmental predictor for temporal changes in biological time series (Kahru & Mitchell, 2000; Mackas et al., 2001). We anticipate its utility as an ecological index will continue to be examined in future research.

## 5. Conclusions

The NOI and SOI time series are generally similar, but provide distinct perspectives on a range of climate variations. Their disparities result mainly from differences between tropical and Northern Hemisphere extratropical variability on interannual scales, which are the result of such things as differences in the proximity and strength of major energy sources for climatic variations (e.g. western tropical Pacific warm pool, Asian monsoon region, subtropical jets, NEP ocean temperature anomalies). A number of studies have shown that the SOI is strongly correlated with many environmental and biological parameters in the NEP. This correspondence may be more a product of the general correlation of SLP in the Asia-Pacific region to the NEP (cf. Fig. 2a) than to a direct physical link. Both the NOI and the SOI have merits, but for the NEP, the NOI appears to be equal or superior in terms of statistical correlations, and a more relevant index of the physical mechanisms responsible for environmental variability.

The NPH is a major link between the atmosphere and ocean in the NEP. Because of the role of the NPH in the H-W circulation, its variations are a good indicator of the impacts of large-scale climate change on the NEP. NPH variations also summarize the regional mechanisms responsible for oceanic anomalies in the NEP, since they are linked closely to the surface winds that drive oceanic processes. Thus an index based on the NPH is likely to be well correlated with climate change events over the North Pacific-North American region, including a wide range of upper ocean changes in the NEP.

Because the ocean in the NEP responds to regional atmospheric forcing as well as to teleconnections from the tropical Pacific, the NOI embodies both local and remote forcing mechanisms, and therefore represents more sources of variation in the NEP than a purely tropically or extratropically based index (e.g. the SOI or NPH alone). Climate processes known to have large physical and biological impacts on the NEP are well represented by the NOI. The encouraging relationships between the NOI and a variety

of physical and biological data series suggests this index may be a reliable indicator of climate fluctuations in the NEP, and provides insights on the mechanisms linking the physical environment to marine resources.

## Acknowledgements

The authors thank Cathy Smith, NOAA-CIRES Climate Diagnostics Center, for developing the global fields and methods used to compute the global correlation maps. These figures are based on data provided by the NOAA-CIRES Climate Diagnostics Center, Boulder, CO from their web site at <http://www.cdc.noaa.gov/>. Lynn deWitt, Chris Moore and Steve Cummings of the Pacific Fisheries Environmental Laboratory (PFEL) and Pete Braccio of the Naval Postgraduate School (NPS) assisted in preparing this manuscript. Roy Mendelsohn, Richard Parrish and Grigory Monterey of PFEL and Grant Cooper of NPS, and two anonymous reviewers provided many useful comments and critiques. We thank the number of researchers who have provided us feedback on the utility of these indices to their specific studies. This research was funded as part of the US GLOBEC Northeast Pacific Project, with support from the NSF Division of Ocean Sciences and the NOAA Coastal Ocean Program Office, and by the salmon research program of the NOAA-NMFS Pacific Fisheries Environmental Laboratory. This is contribution number 195 of the US GLOBEC Program, jointly funded by the National Science Foundation and the National Oceanic and Atmospheric Administration.

## References

- Barnston, A. G., & Livezey, R. E. (1987). Classification, seasonality and persistence of low-frequency atmospheric circulation patterns. *Monthly Weather Review*, *115*, 1083–1126.
- Beamish, R. J. (1993). Climate and exceptional fish production off the west coast of North America. *Canadian Journal of Fisheries and Aquatic Science*, *50*, 2270–2291.
- Bjerknes, J. (1966). A possible response of the atmospheric Hadley circulation to equatorial anomalies of ocean temperature. *Tellus*, *18*, 820–829.
- Bjerknes, J. (1969). Atmospheric teleconnections from the equatorial Pacific. *Monthly Weather Review*, *97*, 163–172.
- Brodeur, R. D., & Ware, D. M. (1992). Long-term variability in zooplankton biomass in the subarctic Pacific Ocean. *Fisheries Oceanography*, *1*, 32–38.
- Cayan, D. R. (1992). Latent and sensible heat flux anomalies over the northern oceans. *Journal of Climate*, *5*, 354–369.
- Chelliah, M. (1990). The global climate for June–August 1989: a season of near normal conditions in the tropical Pacific. *Journal of Climate*, *3*, 138–162.
- Chen, W. Y. (1982). Assessment of Southern Oscillation sea-level pressure indices. *Monthly Weather Review*, *110*, 800–807.
- Clarke, A. J., & Lebedev, A. (1999). Remotely driven decadal and longer changes in coastal Pacific waters of the Americas. *Journal of Physical Oceanography*, *29*, 828–835.
- Deser, C., Alexander, M. A., & Timlin, M. S. (1996). Upper ocean thermal variations in the North Pacific during 1970–1991. *Journal of Climate*, *9*, 1840–1855.
- Ebbesmeyer, C. C., Cayan, D. R., McLain, D. R., Nichols, F. H., Peterson, D. H., & Redmond, K. T. (1991). 1976 step in the Pacific climate: Forty environmental changes between 1968–1975 and 1977–1984. In J. Betancourt, & V. L. Sharp (Eds.), *Proceedings of the 7th Annual Pacific Climate Workshop* (pp. 29–141). (California Department of Water Resources, Interagency Ecology Study Program Technical Report, 26).
- Finney, B. P., Gregory-Eaves, I., Sweetman, J., Douglas, M. S. V., & Smol, J. P. (2000). Impacts of climatic change and fishing on Pacific salmon abundance over the past 300 years. *Science*, *290*, 795–799.
- Ford, B. (2000). *El Niño, La Niña effects on Tropical Cyclones: The Mechanisms*. M.S. Thesis, Naval Postgraduate School, Monterey CA.
- Francis, R. C., & Hare, S. R. (1994). Decadal-scale regime shifts in the large marine ecosystems of the Northeast Pacific: A case for historical science. *Fisheries Oceanography*, *3*, 279–291.
- Gill, A. E. (1982). *Atmosphere–Ocean dynamics*. San Diego, CA: Academic Press.
- Hadley, G. (1735). Concerning the cause of the general trade-winds. *Philosophical Transactions of the Royal Society of London*, *39*, 58–62.

- Horel, J., & Wallace, J. M. (1981). Planetary-scale atmospheric phenomena associated with the Southern Oscillation. *Monthly Weather Review*, *109*, 813–829.
- Hoskins, B., & Karoly, D. (1981). The steady linear response of a spherical atmosphere to thermal and orographic forcing. *Journal of Atmospheric Science*, *38*, 1179–1196.
- Hurrell, J. W. (1995). Decadal trends in the North Atlantic Oscillation: Regional temperatures and precipitation. *Science*, *269*, 676–679.
- Jacobs, G. A., Hurlburt, H. E., Kindle, J. C., Metzger, E. J., Mitchell, J. L., Teague, W. J., & Wallcraft, A. J. (1994). Decade-scale trans-Pacific propagation and warming effects of an El Niño anomaly. *Nature (London)*, *370*, 360–363.
- Kahru, M., & Mitchell, B. G. (2000). Influence of the 1997–98 El Niño on the surface chlorophyll in the California Current. *Geophysical Research Letters*, *27*, 2937–2940.
- Kalnay, E. et al. (1996). The NCEP/NCAR Reanalysis 40-year Project. *Bulletin of the American Meteorological Society*, *77*, 437–471.
- Knutson, T., & Manabe, S. (1998). Model assessment of decadal variability and trends in the tropical Pacific Ocean. *Journal of Climate*, *11*, 2273–2296.
- Knutson, T., & Weickmann, K. (1987). 30–60 day atmospheric oscillations: composite life cycles of convection and circulation anomalies. *Monthly Weather Review*, *115*, 1407–1436.
- Levitus, S., Boyer, T. P., Conkright, M. E., O'Brien, T., Antonov, J., Stephens, C., Stathoplos, L., Johnson, D., & Gelfeld, R. (1998). In *NOAA Atlas, NESDIS 18, World Ocean Data Base, 1998: Vol. 1: Introduction* (p. 346). Washington, D.C.: U.S. Government Printing Office.
- Mackas, D. L., Thomson, R. E., & Galbraith, M. (2001). Changes in the zooplankton community of the British Columbia continental margin, and covariation with oceanographic conditions, 1985–1998. *Canadian Journal of Fisheries and Aquatic Science*, *58*, 685–702.
- Mantua, N., Hare, S., Zhang, Y., Wallace, J., & Francis, R. (1997). A Pacific interdecadal climate oscillation with impacts on salmon production. *Bulletin of the American Meteorological Society*, *78*, 1069–1079.
- McAlpin, J. D. (1995). Rossby wave generation by poleward propagating Kelvin waves: The midlatitude quasigeostrophic approximation. *Journal of Physical Oceanography*, *25*, 1415–1425.
- McFarlane, G. A., King, J. R., & Beamish, R. J. (2000). Have there been recent changes in climate? Ask the fish. *Progress in Oceanography*, *47*, 147–169.
- McPhaden, M. J., & Yu, X. (1999). Equatorial waves and the 1997–98 El Niño. *Geophysical Research Letters*, *26*, 2961–2964.
- Meehl, G. A. (1997). The south Asian monsoon and the tropospheric biennial oscillation. *Journal of Climate*, *10*, 1921–1943.
- Miller, A. J., Cayan, D. C., Barnett, T. P., Graham, N. E., & Oberhuber, J. M. (1994). Interdecadal variability of the Pacific Ocean: Model response to observed heat flux and wind stress anomalies. *Climate Dynamics*, *9*, 287–302.
- Miller, A. J., & Schneider, N. (2000). Interdecadal climate regime dynamics in the North Pacific Ocean: Theories, observations and ecosystem impacts. *Progress in Oceanography*, *47*, 355–379.
- Murphree, T., & Reynolds, C. (1995). El Niño and La Niña effects on the northeast Pacific: The 1991–1993 and 1988–1989 events. *California Cooperative Oceanic Fisheries Investigations Reports*, *36*, 45–56.
- Mysak, L. (1986). El Niño, interannual variability and fisheries in the northeast Pacific Ocean. *Canadian Journal of Fisheries and Aquatic Science*, *43*, 464–497.
- Nitta, T. (1987). Convective activities in the tropical western Pacific and their impact on the Northern Hemisphere summer circulation. *Journal of the Meteorological Society of Japan*, *65*, 373–390.
- Nitta, T., & Yamada, S. (1989). Recent warming of tropical sea surface temperature and its relationship to the Northern Hemisphere circulation. *Journal of the Meteorological Society of Japan*, *67*, 375–383.
- Pares-Sierra, A., & O'Brien, J. (1989). The seasonal and interannual variability of the California Current System: A numerical model. *Journal of Geophysical Research*, *94*, 3159–3180.
- Parrish, R. H., Schwing, F. B., & Mendelsohn, R. (2000). Midlatitude wind stress: The energy source for climatic regimes in the North Pacific Ocean. *Fisheries Oceanography*, *9*, 224–238.
- Peixoto, J., & Oort, A. (1992). *Physics of climate*. Woodbury, NY: American Institute of Physics.
- Philander, G. (1990). *El Niño, La Niña and the Southern Oscillation*. San Diego, CA: Academic Press.
- Polovina, J. J., Mitchum, G. T., Graham, N. E., Craig, M. P., DeMartini, E. E., & Flint, E. N. (1994). Physical and biological consequences of a climate event in the central North Pacific. *Fisheries Oceanography*, *3*, 15–21.
- Pulwarty, R., & Redmond, K. (1997). Climate and salmon restoration in the Columbia River basin: The role and usability of seasonal forecasts. *Bulletin of the American Meteorological Society*, *78*, 381–397.
- Redmond, K. T., & Koch, R. W. (1991). Surface climate and streamflow variability in the western United States and their relationship to large-scale circulation indices. *Water Resources Research*, *27*, 2381–2399.
- Reynolds, C., Gelaro, R., & Murphree, T. (1996). Observed and simulated Northern Hemisphere intraseasonal circulation anomalies and the influence of model bias. *Monthly Weather Review*, *124*, 1100–1118.
- Roemmich, D., & McGowan, J. (1995). Climatic warming and the decline of zooplankton in the California Current. *Science*, *267*, 1324–1326.

- Schwing, F., Moore, C., Ralston, S., & Sakuma, K. A. (2000). Record coastal upwelling in the California Current in 1999. *California Cooperative Oceanic Fisheries Investigations Reports*, 41, 148–160.
- Schwing, F. B., Murphree, T., deWitt, L. & Green, P. M. The evolution of oceanic and atmospheric anomalies in the northeast Pacific during the El Niño and La Niña Events of 1995–2001. *Progress in Oceanography*, 54, (in press).
- Sette, O. E., & Isaacs, J. D. (1960). Symposium on the changing Pacific Ocean in 1957 and 1958. *California Cooperative Oceanic Fisheries Investigations Reports*, 7, 13–217.
- Simpson, J. J. (1992). Response of the southern California Current system to the mid-latitude North Pacific coastal warming events of 1982–1983 and 1940–1941. *Fisheries Oceanography*, 1, 57–79.
- Strub, P. T., & James, C. (2002). Altimeter-derived surface circulation in the large-scale NE Pacific gyres: Part 2. 1997-1998 El Niño anomalies. *Progress in Oceanography*, 53(2-4), 185–214.
- Trenberth, K. E. (1990). Recent observed interdecadal climate changes in the Northern Hemisphere. *Bulletin of the American Meteorological Society*, 71, 988–993.
- Trenberth, K. E., & Hurrell, J. W. (1994). Decadal atmospheric-ocean variations in the Pacific. *Climate Dynamics*, 9, 303–319.
- Trenberth, K. E., & Shea, D. J. (1987). On the evolution of the Southern Oscillation. *Monthly Weather Review*, 115, 3078–3096.
- Walker, G. T. (1924). Correlation in seasonal variations of weather. IX. A further study of world weather. *Memoirs of the Indian Meteorological Department*, 24, 275–332.
- Wooster, W.S., & Fluharty, D.L. (Eds.). (1985). *El Niño North: Niño Effects in the Eastern Subarctic Pacific Ocean*. Seattle, WA: Washington Sea Grant Program.